Study on a High-Power Stirling Cryocooler

Y. Xu, Y. C. Cai, D. M. Sun, Q. Shen, X. Zhao, J. Zhang, Z. Z. Cheng

Institute of Refrigeration and Cryogenics, Zhejiang University,
Hangzhou, P. R. China 310027

ABSTRACT

Stirling cryocoolers are well-adapted to high temperature superconductivity application and small scale gas liquefaction, due to their high efficiency, wide operating temperature range and fast cool-down process. A high-power Stirling cryocooler driven by a crank-rod mechanism was designed by SAGE-software, built and tested systematically. The cooling performance of the cryocooler is analyzed under various operating conditions. A cooling power of 640.5 W at 77 K with an electric input power of 11 kW has been achieved. The comparison analysis between SAGE-model and experimental results has shown the direction for further design optimization of the high-power Stirling cryocooler.

INTRODUCTION

The high-power cryocooler is an important bridge between cryogenic technology and industrial application. Urgent requirements of high temperature superconducting (HTS) technology and small scale gas liquefaction have spurred the rapid development of high-power cryocoolers. Taking superconductors as an example, YBCO wires, known as the 2nd generation superconducting wire, show more prominent current-carrying performance at liquid nitrogen temperature. An important trend shows more prominent current-carrying performance at liquid nitrogen temperature [1]. Application of YBCO wires enable HTS power devices to work at higher cryogenic temperatures, thus further encouraging the opportunity to develop cryocoolers operating at the temperature of liquid nitrogen [2].

At present, the main types of cryocooler aimed at high power and liquid nitrogen temperatures are Stirling cryocoolers, Gifford-McMahon (GM) cryocoolers [3] and pulse tube cryocoolers (PTC) [4]. Stirling cryocooler features high efficiency, fast cool-down, a wide range of refrigeration temperature, and kilowatt cooling capacity. Combined with mature manufacturing technology and low cost, the Stirling cryocooler driven by crank-rod mechanisms is an important industrial cryocooler which is widely applied in low temperature liquefaction. The GM cryocooler is initially developed to obtain extremely low temperature. Its industrial application is limited by low efficiency, restricted cooling capacity and specific technical requirements. Stirling-type PTCs have a long life span, due to the elimination of moving parts in the cold end of traditional Stirling cryocooler. High efficiency can be usually obtained in small-scale Stirling-type PTCs with a cooling capacity less than 10 W. However, efficiency of large scale Stirling-type PTC is still lower than expected, since inhomogeneous flow and temperature severely deteriorates cooling performance [5]. Consequently, although traditional Stirling cryocoolers have

Cryocoolers 18, edited by S.D. Miller and R.G. Ross, Jr.

some drawbacks, the excellent cooling performance and relative mature manufacturing technology make it the best and economical candidate for kilowatt-class cooling applications.

In this paper, a high-power Stirling cryocooler driven by a crank-rod mechanism was simulated, developed and tested systematically.

EXPERIMENTAL SYSTEM

Experimental Setup

Figure 1 shows the schematic view of the Stirling cryocooler test system. The Stirling cryocooler can be divided into two major parts, i.e. the driver module and the refrigeration module. As shown in Figure 1, the driver module consists of a three-phase asynchronous motor, oil pump and crank-rod mechanism that connects with a compression piston and a displacer.

The refrigeration module consists of a compression space, an ambient heat exchanger, a regenerator, a cold heat exchanger and an expansion space. In the Stirling cryocooler, the ambient heat exchanger is the most heavily heat loaded component. To achieve large heat exchange capacity and compactness simultaneously, a shell-and-tube heat exchanger is used in the experiment. As this type of heat exchanger has a large heat transfer area and small volume, it can minimize the compressor dead volume and avoid excessive acoustic power dissipation caused by the pressure drop [6]. The number of small gas tubes already reaches 216 for the design heat load of ~10 kW. A low pressure drop and a large surface area are also important for the cold heat exchanger. The cold heat exchanger is a slit-type heat exchanger that has 160 channels; each with a small cross section. The regenerator is packed with randomly arranged copper fiber with a diameter of 16 μm, and has excellent thermal conductivity.

The cold heat exchanger and the regenerator of the Stirling cryocooler are wrapped by multi-layer thermal insulation material and placed in a vacuum chamber.

In the simulation and experiment, the working gas is high purity helium. Chill water with an initial temperature of 288 K and a steady flow rate of 1 m^3/h is supplied to cool down the ambient heat exchanger and the water jacket around the compression cylinder. Table 1 shows the main parameters of the Stirling cryocooler.

The heat balance method is used to measure cooling capacity. A group of electric resistances are evenly mounted around the cold heat exchanger to mimic the thermal load. Thermal load, i.e. the cooling power, is adjusted by changing the voltage across an electric resistance and is displayed by a digital power meter. A calibrated Pt100 temperature sensor with an accuracy of ± 0.1 K is used to measure the cold end temperature.

A model 511.940 Huba pressure sensor is installed to monitor pressure oscillations in the compression space. The hardware devices of the data acquisition system are supplied by National Instrument Corporation, including the data acquisition card PCI-6220, terminal box SCB-68, and shield wires SHC68-68-EPM. Two packaged Pt100 sensors and a water flow meter measure the inlet and outlet temperatures and the instantaneous flow rate of the chilled water, respectively. An experimental data acquisition program utilizes LabVIEW 2009 [7].

PERFORMANCE AND DISCUSSION

Cool-down Curves

Figure 2 shows a typical cool down curve with a charge pressure of 1.8 MPa, an input electric power of 11 kW and a rotating speed of 1450 r/min. It takes about 6 minutes for the cold head to cool down from the ambient temperature to the minimum no-load temperature of 54.08 K. As the cooler continues running, the no-load temperature is finally stabilized at about 55.2 K. The cool down time is about 4.47 min to reach a temperature of 77 K (liquid Nitrogen) and about 3.52 min to reach temperature of 110 K (Liquid Natural Gas). In contrast, a high power Stirling type PTC needs more than 20 minutes to reach 77 K [8]. When the Stirling cryocooler reaches a stable operation state without heat load, the cold end temperature is monitored continuously. As shown in Figure 3, the cold end temperature varies within $\pm$ 0.13 K.

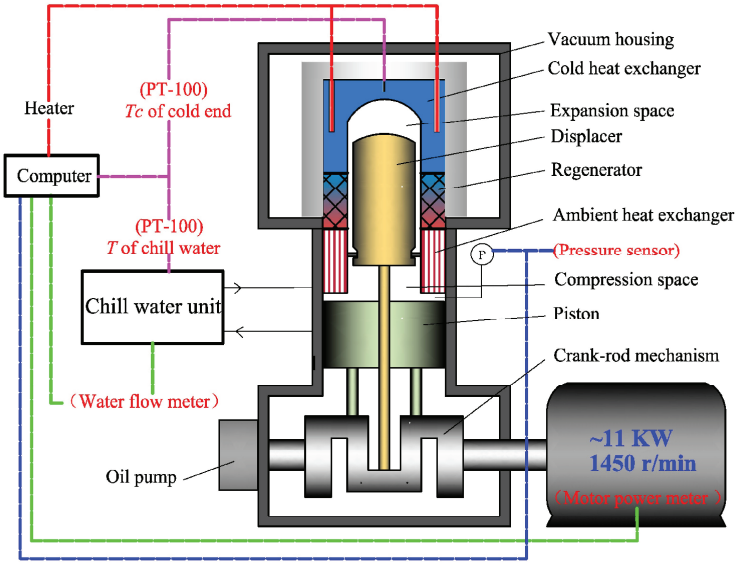

Figure 1. Schematic of the Stirling cryocooler.

Table 1. Main dimensions of the Stirling cryocooler

Compression piston	Diameter: 80 mm, stroke: 52 mm
Expansion piston	Diameter: 76 mm, stroke: 30 mm
Regenerator	Outer diameter: 102 mm, inner diameter: 76 mm, length: 46.5 mm
Motor	Rated power: 11 kW, rated rotating speed: 1450 r/min

The cooling power rises with an increase in charging pressure. Considering the safe operation of the Stirling cryocooler, the maximum charging pressure in the experiment is 1.8 MPa. When the charging pressure is increased from 1.2 MPa to 1.7 MPa, the cool-down time to reach a no-load refrigeration temperature of 77 K decreases from 6.25 min to 4.47 min as seen in Fig. 4. According to this trend of a relatively high charging pressure, the cool down time remains almost constant. The experimental results demonstrate the characteristics of fast cool-down and stable operation of the Stirling cryocooler.

Load Curves

Figure 5 shows the load curves of the Stirling cryocooler with a working pressure of 2.65 MPa and the crankshaft rotating speed of 1450 r/min. The cooler reaches no-load refrigeration

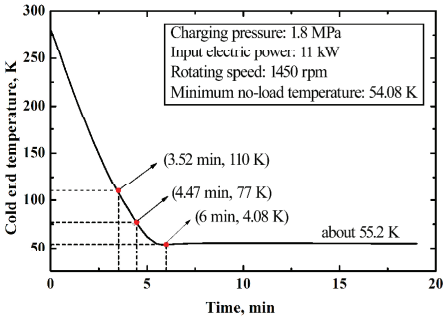

Figure 2. Cool-down curve of the Stirling cryocooler.

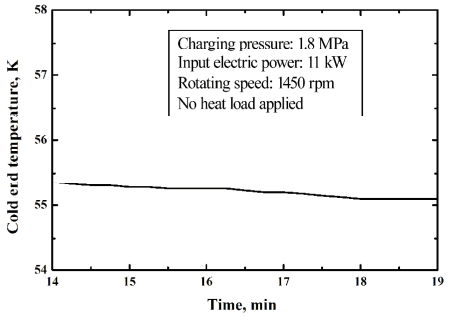

Figure 3. Temperature stability of the Stirling cryocooler.

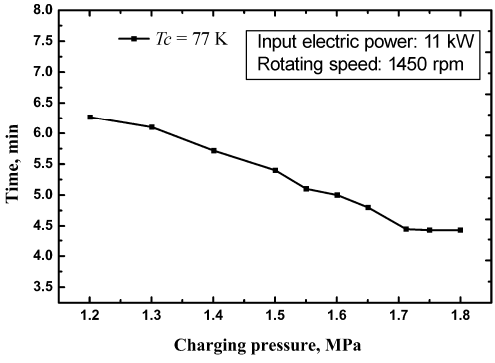

Figure 4. Cool-down time at different charging pressure.

temperature of 49.1 K, and provides 636 W cooling power at about 77 K. In the SAGE simulation, the no-load refrigeration temperature is much lower; reaching 29.5 K, and the corresponding cooling power at 77 K is 1020 W. The simulation load curve has the same trend as the experimental one. Besides unavoidable calculation error, there are possible reasons for the discrepancy: (1) the working medium (helium) is susceptible to oil pollution because this type of driving mechanism needs oil lubrication. Since oil accumulates in the regenerator, cooling performance will get worse. However, in the SAGE model, this type of performance deterioration is neglected, (2) power consumption increases because of some frictional dissipations which usually occur in the clearance between the compression piston and cylinder, the junction between the crank shaft and connecting rods, and crankshaft gears.

The performance of the Stirling cryocooler is strongly influenced by the charging pressure. The charging pressure is the system equilibrium pressure before the Stirling cryocooler starts.

Since a balance reservoir exists in the system, the operating pressure will be much higher that the charging pressure because the average temperature rises during operation. For example, corresponding to ae charging pressure of 1.65 MPa, the mean operating pressure will reach 2.65 MPa during run time. Figure 6 shows the load curves at different charging pressure. As the charging pressure is increased from 1.2 MPa to 1.8 MPa, the cooling power at 77 K rises from 475.2 W to 640.5 W, and the no-load refrigeration temperature gradually increases. Meanwhile, the corresponding COP decreases from 5.74 % to 5.29 % since much more power is consumed at higher charging pressure. The amount of rejected heat from the compression parts of the cooler can indicate it. Figure 7 and 8 show variations of rejected heat from the water jacket and the ambient heat exchanger at different charging pressure, respectively. At the higher charging pressure, there is much more heat generated in compression parts and, meanwhile, taken away by the chill water. As shown, the rejected heat from water jacket around cylinder, which is

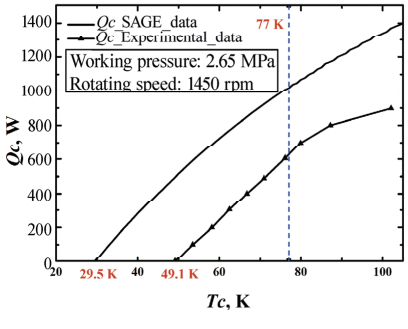

Figure 5. Load curve at mean pressure of 2.65 MPa

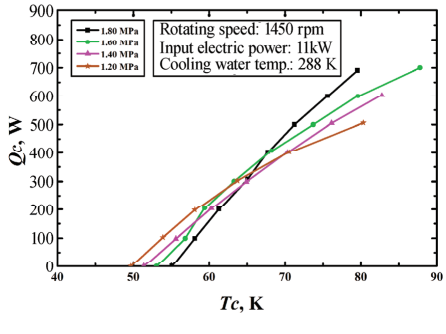

Figure 6. Load curves at different charging pressure

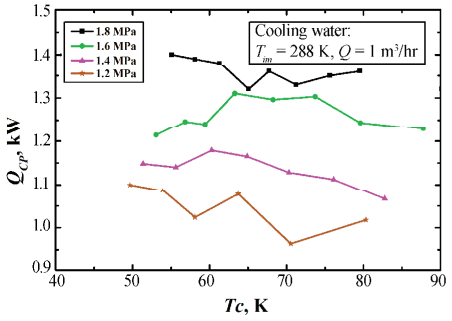

Figure 7. Rejected heat from water jacket around cylinder at different charging pressure.

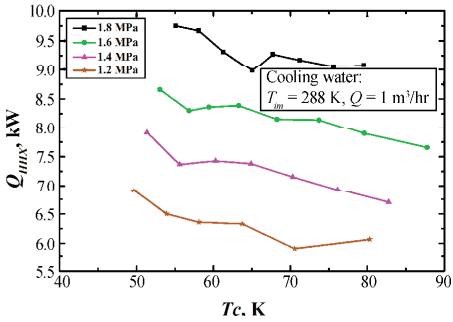

Figure 8. Rejected heat from hot heat exchanger at different charging pressure.

only a small portion of the total heat generation, is in the small range of 1.0~1.4 kW. However, the rejected heat from the ambient heat exchanger increases significantly with the charging pressure, and almost reaches 9.1 kW at 77 K and 1.8 MPa. Based on the variation trend presented in Fig. 8, it is apparent that the ambient heat exchanger has enough heat dissipation capacity under the present pressure range.

CONCLUSIONS

A high-power Stirling cryocooler driven by a crank-rod mechanism is developed and tested. A cooling power of 640.5 W at 77 K has been achieved with the electric input power of 11 kW when the charging pressure is 1.8 MPa. A large deviation between the experimental results and the SAGE model is found, which is primarily caused by internal gas contamination and the mechanism wear. Effects of the charging pressure on the cooling performance and the rejected heat in the ambient end are analyzed. These results fully indicate the advantage of Stirling cryocooler, such as fast cool-down, large cooling capacity and high efficiency, and lay an experimental foundation for future optimization.

ACKNOWLEDGMENT

This work is financially supported by National Natural Science Foundation of China (No. 51276156) and State Key Development Program for Basic Research of China (No. 2010CB227303).

REFERENCES

1. Paranthaman, M.P., Izumi, T., “High-performance YBCO-coated Superconductor Wires,” *MRS Bulletin*, Vol. 29, No. 28 (2004), pp. 533-541.
2. Hirai, H., Suzuki, Y., Hirokawa, M., et al., “Development of a Turbine Cryocooler for High Temperature Superconductor Applications”. *Physica C: Superconductivity*, Vol. 469, No. 15-20(2009), pp. 1857-1861.
3. Chang, H., Ryu, S., and Kim, M., “Performance of Heat Exchanger for Subcooling Liquid Nitrogen with a GM Cryocooler”, *Adv. in Cryogenic Engineering*, Vol. 55, Amer. Institute of Physics, Melville, NY (2010), pp. 345-352.
4. Chen, R.L., Henzler, G., Royal, J., et al., “Reliability Test of a 1 - kW Pulse Tube Cryocooler for HTS Cable Application,” *Adv. in Cryogenic Engineering*, Vol. 55, Amer. Institute of Physics, Melville, NY (2010), pp. 727-735.
5. Sun, D.M., Dietrich, M., and Thummes, G., “High-power Stirling-type Pulse Tube Cooler Working below 30K”, *Cryogenics*, Vol. 49, No. 9 (2009), pp. 457-462.

6. Martin, J.L., Martin, C.M., "Pulse tube cryocoolers for industrial applications," *Adv. in Cryogenic Engineering*, Vol. 47B, Amer. Institute of Physics, Melville, NY (2002), pp. 662-669.

7. LabVIEW User Manual, National Instruments, Austin, TX, 2009.

8. Sun, D.M., Dietrich, M., and Thummes, G., "Investigation on High-Power Stirling-Type Pulse Tube Coolers for Cooling HTS Motors," *IEEE Trans. on Applied Superconductivity*, Vol. 22, No. 3 (2012).